Journal of the Optical Society of America A
OPTICS, IMAGE SCIENCE, AND VISION

SPICA, Stellar Parameters and Images with a Cophased Array: a 6T visible combiner for the CHARA array

Denis Mourard,[1,*] Philippe Bério,[1] Karine Perraut,[2] Jean-Michel Clausse,[1] Orlagh Creevey,[1] Marc-Antoine Martinod,[1] Anthony Meilland,[1] Florentin Millour,[1] and Nicolas Nardetto[1]

[1]Université Côte d'Azur, OCA, CNRS, Lagrange, Parc Valrose, Bât. Fizeau, 06108 Nice cedex 02, France
[2]Université Grenoble Alpes, CNRS, IPAG, 38000 Grenoble, France
*Corresponding author: denis.mourard@oca.eu

Received 5 October 2016; revised 2 February 2017; accepted 10 March 2017; posted 13 March 2017 (Doc. ID 277935); published 3 April 2017

High angular resolution studies of stars in the optical domain have highly progressed in recent years. After the results obtained with the visible instrument Visible spEctroGraph and polArimeter (VEGA) on the Center for High Angular Resolution Astronomy (CHARA) array and the recent developments on adaptive optics and fibered interferometry, we have started the design and study of a new six-telescope visible combiner with single-mode fibers. It is designed as a low spectral resolution instrument for the measurement of the angular diameter of stars to make a major step forward in terms of magnitude and precision with respect to the present situation. For a large sample of bright stars, a medium spectral resolution mode will allow unprecedented spectral imaging of stellar surfaces and environments for higher accuracy on stellar/planetary parameters. To reach the ultimate performance of the instrument in terms of limiting magnitude (Rmag $\simeq$ 8 for diameter measurements and Rmag $\simeq$ 4 to 5 for imaging), Stellar Parameters and Images with a Cophased Array (SPICA) includes the development of a dedicated fringe tracking system in the H band to reach "long" (200 ms to 30 s) exposures of the fringe signal in the visible.

OCIS codes: (120.3180) Interferometry; (120.4640) Optical instruments.

https://doi.org/10.1364/JOSAA.34.000A37

1. INTRODUCTION

In 1974 using the principle of aperture synthesis, Antoine Labeyrie [1] demonstrated the direct and coherent combination of light collected by two separate telescopes. This fundamental achievement opened the road for "unlimited" angular resolution, or at least resolution well beyond the diffraction limit of the largest telescopes. In the next decade, 30–40 m class telescopes will have their first light but optical interferometers operating today are already well below the diffraction limit of these giants. In the 1970s and early 1980s, optical interferometry was developed in the visible domain (I2T [1], MarkIII [2], GI2T [3], SUSI [4], COAST [5], NPOI [6]). The performance of detectors was really superior in the visible domain at that time, but rapid progress in infrared detectors and the advantage of working at longer wavelengths to minimize the effects of the atmospheric turbulence have progressively led to faster developments of optical interferometers in the infrared domain. The 1990s was the great age of IOTA, then PTI [7] and the progressive apparition of the giants VLTI [8] and KECK-I [9], both designed at the beginning for near- and mid-infrared operations. GI2T, NPOI, and SUSI were still continuing their development but mainly on very dedicated programs. The arrival of the CHARA array [10] in the early 2000s opened a very interesting opportunity for collaborative developments of interferometric instruments. With the first generation of instruments on the VLTI the 2000s led to the progressive closing of "small" installations (COAST, IOTA, PTI, GI2T, SUSI) and a concentration of efforts on VLTI, CHARA, and KECK-I. Today CHARA and VLTI are the only two large facilities. NPOI is evolving toward extended imaging capabilities and MROI [11] is in the construction phase. The ends of the 2000s and the 2010s saw the fabulous arrival of images, as was so long expected by the pioneers. Even though the infrared is dominating the domain, visible instruments are productive and produce unique data and scientific results thanks to the higher angular resolution and the long tradition of coupling angular and spectral resolution.

In this paper, we present the recent developments made on the CHARA array from VEGA [12,13] to FRIEND [14] (Section 2). We describe then in detail the studies that we have started for a future six-telescope (6T) visible combiner

(Section 3), and finally we present preliminary considerations for the requirements and specifications of an infrared fringe tracker to assist the visible instrument in Section 4.

2. FROM VEGA TO SPICA

VEGA is one of the two visible instruments of the CHARA array, along with PAVO [15]. PAVO is a two- or three-telescope combiner where fringes are formed in the pupil plane. An integral field spectrograph is located in this pupil plane to sample the 650–800 nm domain over 15 spectral channels and numerous subapertures on the pupil using an EMCCD. It has been designed for observing faint stars (Rmag around 8), with accurate visibility measurements for precise determinations of diameters [16,17] and limb darkening measurements [18]. The slicing of the pupil by the integral field unit acts as a spatial filtering permitting high precision visibility measurements. PAVO, as VEGA, can benefit from the assistance of group delay tracking by one of the infrared instruments, usually CLIMB [19] or, sometimes, MIRC [20].

VEGA can operate in 2T, 3T, or 4T mode. It is equipped with a spectrograph for low (R = 1700), medium (R = 5000), and high (R = 30, 000) spectral resolution. In medium and high resolution, two separate photon-counting detectors based on intensified CCD record two separate spectral domains, separated by 140 nm (resp. 30 nm) in medium (resp. high) resolution. VEGA recombines the telescope beams in an image plane where the entrance slit of the spectrograph is located. Therefore this instrument is sensitive to the speckle noise of the atmospheric turbulence and thus works in a multimode regime [3].

The early years of astrophysical exploitation of VEGA have confirmed its scientific potential with 33 publications in different fields of stellar physics: fundamental parameters, stellar atmospheres, and circumstellar environments. The first polychromatic (across the H α line) reconstructed image of the circumstellar disk around the Be star ϕ Per has been obtained recently [21]. Despite this potential, we have also understood the current limitations of VEGA that are mainly due to the multi-speckle mode and the use of a photon-counting detector with an intensified CCD. The first issue leads to a dilution of the incoming flux in the different speckles, which directly impacts the signal-to-noise ratio (S/N hereafter) and therefore the limiting magnitude. This is true on squared visibility or differential visibility but it becomes even more critical on higher-order observables such as the closure phase [22]. The photon-counting detectors [23] developed at Observatoire de la Côte d'Azur and Observatoire de Lyon more than 10 years ago have a much lower dark current ($\sim 5 \times 10^{-6} e^-$/pixel/frame) than the current number for the EMCCD [dark current $\sim 4 \times 10^{-6} e^-$/pixel/frame and clock-induced charge (CIC)$\sim 1 \times 10^{-3} e^-$/pixel/frame]. Despite their better quantum efficiency (~90% versus ~30%), the 200-times larger dark current of the EMCCD detectors limits their performance for fringe measurements at very low flux. The intensified photon-counting detectors are, however, limited by the effect of saturation at high flux regime in the intensified microchannels and by the effect of the photon centroiding hole [24], preventing close pairs of photo events to be detected. These two limitations lead to difficulties to measure unbiased low visibilities ($V < 0.2$) and to define a reliable estimator of the closure phase.

Two major progresses have recently changed the situation. First, the recent advances in low-noise detectors (new generation of EMCCDs) permit their use in photon-counting regimes without the photon centroiding hole. Second, the CHARA telescopes will be soon equipped with adaptive optics (AO) systems [25,26] permitting a Strehl ratio of 83% in the H band and around 20%–25% in the visible domain. The principle of spatial filtering by the use of single-mode optical fibers can, therefore, be applied in the visible domain as has been done in the near-infrared and with a reasonable coupling efficiency. We have thus developed a demonstrator instrument called FRIEND [14] that combines the beams coming from three telescopes by applying a spatial filtering with single-mode optical fibers (see Fig. 1). It operates in the R spectral band (from 600 to 750 nm) and uses a low-noise and fast readout EMCCD camera, OCAM^2 [27]. This instrument is installed on the VEGA table and it allows us to test various aspects of a future six-telescope visible interferometric instrument.

After a few months of tests and operation, we have been able to validate the concept even without the AO system in operation on the CHARA telescopes. In a recent paper [28] we have described the numerical model of the instrument and the associated data reduction software for squared visibility and closure phase measurements. This model and the first data have permitted calibration of our S/N calculator. Without the AO systems, the coupling efficiency in the fibers is very low in the visible (of the order of 1%) and this prevents us from measuring differential complex visibilities on narrow spectral bands with a

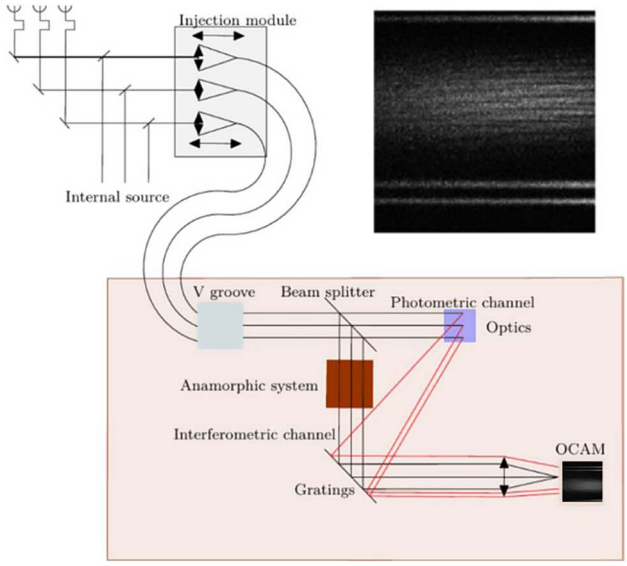

Fig. 1. Schematic representation of the FRIEND prototype. The telescopes and delay lines are represented in the upper-left part of the figure. They feed the injection module and the three single-mode fibers. The beams coming from the telescopes could be replaced by an internal source for alignment and calibration purposes. The output of the fibers is rearranged by a V-groove to form a linear nonredundant pupil. A beam splitter sends 70% of the flux to the dispersion grating through an anamorphosis optic for a correct adaptation of the spatial and spectral sampling in the interferometric channel. The remaining 30% are sent to the grating through small individual flat mirrors tilting each of the three beams to separate the photometric channels. The interferometric and photometric channels are then imaged on the detector.

reasonable signal-to-noise ratio. We have also demonstrated the need for correcting the birefringence in the fibers to optimize the instrumental contrast and we have developed and tested a compensation system. The first on-sky observations have permitted a reliable angular diameter determination on a known star and the demonstration of the stability of the transfer function of the instrument, although more data are required to accurately quantify this stability.

The FRIEND prototype was developed with the spirit of paving the way for a future 6T visible beam combiner capitalizing on the successes of VEGA and on the arrival of the AO system on the CHARA array. SPICA is, in its instrumental principles, an extension of FRIEND to 6T but it is considered, of course, as a full scientific instrument with all the efforts put on improving the reliability, the sensitivity, the robustness, and the observing efficiency for fulfilling its science objectives.

3. SPICA DEVELOPMENTS

A. Main Science Cases

Our main science case concerns the measurements of the angular diameter of main sequence stars of solar type stars or later (G,K) on a sufficiently large sample. For the sky accessible to CHARA ($\delta > -20°$) and according to the SIMBAD database at CDS, the number of (F-G-K) stars is roughly multiplied by 10 in each spectral type if ones goes from a limiting V magnitude of 4–6 and again from 6 to 8 (41-49-70 stars for Vmag < 4, 462-437-818 for Vmag < 6, and 4978-3867-9348 for Vmag < 8). Therefore, this main science goal requires the possibility to reach a magnitude between 6 and 8. In Fig. 2 we present the estimated stellar angular diameter of main sequence stars as a function of the V magnitude and for a certain number of spectral types. From this figure, we can see that measuring these angular diameters in this range of magnitude implies reaching an angular resolution down to 0.1 ms of arc (mas hereafter). With 330 m baselines in the visible ($\lambda = 600$ nm), the angular resolution reaches 0.4 mas but measuring smaller angular diameters is possible by fitting visibility curves for partially resolved objects [30].

The knowledge of stellar properties (R, Teff, M, age) is fundamental in many areas of astronomy, and more recently, thanks to the detection of oscillation in thousands of stars with CoRoT and Kepler, there has been a revival of stellar physics. Basic stellar physics relationships link the radius and the effective temperature to the angular diameter, and using evolution models these quantities help constrain the mass and age. Between the angular diameter and the radius, the role of an accurate distance is central and the data releases of Gaia in the coming months/years will play a crucial role. Additionally, coupling a radius with asteroseismic data for solar-like oscillators can help decouple the seismic mass-radius relation to determine the mass and other relevant parameters governing stellar evolution with even higher precision and more accuracy. In [31,32] the potential and formalism of coupling asteroseismology and interferometry have been studied in detail. It shows that reaching 1% accuracy on the stellar radius with direct methods such as optical interferometry yields strong constraints on the stellar atmospheric and internal structure models of stars.

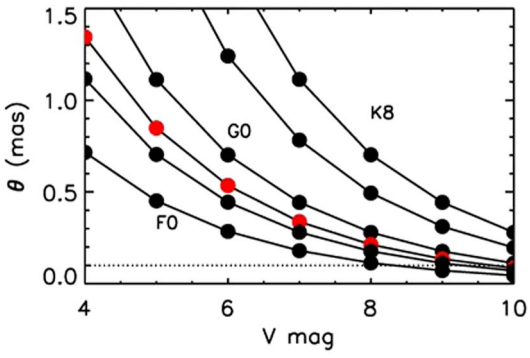

Fig. 2. Angular diameter of zero age main sequence stars of different spectral types and V magnitude, based on expected absolute magnitudes and radii of stars for different spectral types from [29]. Red dots represent a G2 V star. The horizontal line at 0.1 mas represents the angular resolution needed to permit the measurements of F stars up to magnitude 8.

While asteroseismic data have become available for a good sample of stars, independent measures of a large number of radii have not been possible due to the small angular diameter of these fainter stars. In the very recent years photometric space missions (WIRE, MOST, CoRoT, and Kepler) have been providing very long (weeks to months) nearly uninterrupted time series of pulsations in stars all across the HR diagram, and for thousands of giant stars. For many of these targets, direct radius measurements will not be available because of their faintness. But the limitation in exploiting their potential can be overcome by studying their nearby counterparts, for which both angular diameters and seismic data (among others) are available, in particular for testing already existing and developing new surface-brightness or temperature-colors relations, which can be applied directly to these thousands of fainter stars.

The main goals for the next decade in exoplanet science are on the one hand to detect less massive planets, possibly in the habitable zone, and on the other hand, to study in detail the atmospheric properties of larger planets, and better constrain their formation mechanisms. Stellar properties have various impacts in exoplanet searches, especially concerning indirect methods. The limb-darkening coefficient is a necessary input in the simulations of stellar activity. Also, and very importantly, stellar activity (spots and plages at the star surface) produces a stellar jitter that limits planet detection with radial velocities (RV), photometric and astrometric methods. In the case of RV, convection effects may also significantly contribute to the RV jitter. This again limits planet detection capabilities or the precision of the planet's physical/orbital properties when a planet is detected. In some cases it may lead to false detections. RV planet search surveys as well as follow-up of photometric transit surveys thus require a deeper understanding and characterization of the effects of stellar activity to disentangle them from planetary signals. Direct imaging of stellar surfaces may shed light on these false detections and improve the characterization of planets but will require interferometric measurements with a precision better than 0.5%, as demonstrated by [33].

B. General Definition of the Instrument

To achieve these science goals, we propose to study a new visible beam combiner for the CHARA array, called SPICA. It should be designed for the measurement of the angular

diameters of 1000 stars and will provide a major step forward in terms of magnitude and precision with respect to the present situation. The combination of the six CHARA telescopes equipped with AO with a low-resolution spectrograph (50 channels over 600–900 nm) will yield 750 different spatial frequencies in one single observation and thus will allow precise determinations of angular diameters. For a subsample of bright stars, a medium spectral resolution mode (200 channels over 40 nm) will allow spectral imaging of stellar surfaces and environments for higher accuracy on the stellar/planetary parameters and studies on the kinematics of environments and atmospheres. To push the limiting magnitude in the different modes and give access to a large sample of stars, SPICA will require the assistance of a dedicated fringe tracking system in the H band to reach "long" (200 ms–30 s) exposures of the fringe signals in the visible. In the following, we present the concept of the instrument and demonstrate its expected performance.

The SPICA design is based on the FRIEND [14] prototype extended to 6T. A great advantage with a fibered instrument is that the injection module and the instrument itself are completely decoupled. This is not only interesting for implementation but also for the alignment where all the efforts could be focused on the injection system.

The instrument is composed by the modules presented in Fig. 3.

In the injection modules, the light coming from each telescope is focalized into a single-mode polarization-maintaining fiber. Three translation axes on each module permit the optimization of the injection. To avoid losing time on sky for this alignment, which is critical for reaching the overall performance of the instrument, a laser light, at a wavelength different from the science spectral band, is sent back through the fiber in the direction of the CHARA alignment and pupil position controls, which are part of the NCP-AO system (see Section 3.C). The injection modules are installed on linear translation stages, which permit a day-time cophasing of SPICA with the other CHARA instrument.

The second SPICA subsystem is the compensator for the birefringence in the fibers. We have designed a dedicated module for FRIEND based on PIONIER [34] and it was successfully tested on sky in July 2016. This module aims at optimizing the transfer function of the instrument to reach an instrumental visibility of at least 0.9. It is placed either before the injection if one uses transmitting plates for adjusting the differential optical path difference, or directly on the fibers if one uses the principle of fiber twisting.

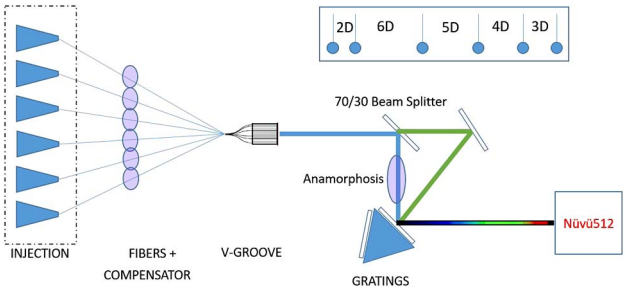

Fig. 3. Schematic layout of the SPICA instrument. The output pupil arrangement at the output of the V-groove is given in the small box.

The photometry extraction is done by a beam splitter (70/30, 30 for the photometry) placed after the V-groove. The beams are then sent to the spectrograph, built around two different gratings for the two spectral resolutions (R = 100, R = 3000). In order to correctly sample the fringes without oversampling the spectral resolution element, an anamorphosis optic is used in the recombined beam (with a magnification of about 25 in the spatial direction perpendicular to the dispersion, see below). Finally, the dispersed combined light and photometric channels are sent to the detector.

For SPICA we have adopted the well-known principle of dispersed fringes with a linear nonredundant reconfiguration of the pupils. The small box in Fig. 3 presents the chosen configuration for the pupil arrangement. The linear arrangement of the six individual pupils is done in a nonredundant way so that each telescope pair has its own spatial frequency on the detector. The proposed spacing B between the six subpupils, expressed in multiple of the output pupil diameter D is (2D-6D-5D-4D-3D). This is the most compact arrangement in 6T and it produces 15 different frequencies (2, 3, 4, 5, 6, 7, 8, 9, 11, 12, 13, 15, 17, 18, 20) to correctly sample the fringe signals coming from the 15 pairs of telescope. To minimize the reduction of the transfer function of the instrument, we consider, like done on VEGA [12] and in the past on the GI2T [3], that the finest fringes (frequency 20) have to be sampled over 6 pixels per fringe. As we will have about 50 fringes of the largest frequency (B = 20D) over the image (2.44B/D) it means that a vertical sampling over 300 pixels minimum is necessary. To accommodate the six photometric channels (which are not concerned by the anamorphosis optics), a detector size of 512 pixels is mandatory. Our choice is for the Nüvü512 detector (see http://www.nuvucameras.com/products/), which today has the best noise level performance (0.1e- per pixel and per frame).

The spectrograph is designed to permit two spectral resolutions to cover the range of scientific programs that will be addressed. First of all we have chosen a low-resolution mode (R = 100) to cover over 50 spectral channels the 600–900 nm spectral band. This mode is for high sensitivity. It will provide 15 V^2 measurements and 10 closure phases in the 50 spectral channels. Even though differential visibilities will also be accessible, their interest will be limited as they will concern spectral channels of 6 nm. In Fig. 4 we present some representative (U,V) plane coverages for three different declinations (0°, 30°, 60° from top to bottom) in the low-resolution mode of SPICA. The (U,V) plane coverage benefits from the 15 baselines, the Earth's rotation, and the spectral sampling. One should of course take into account the intrinsic limitation due to the possible spectral dependence of the object, but the rich frequency coverage will be very useful to improve the accuracy of the diameter determination or for discovery of binary or multiple systems.

Based on the experience acquired with VEGA, we have defined a higher spectral resolution mode, R = 3000, that will allow a simultaneous 40 nm sampling over 200 spectral channels, in the same global range of 600–900 nm. Spectral line

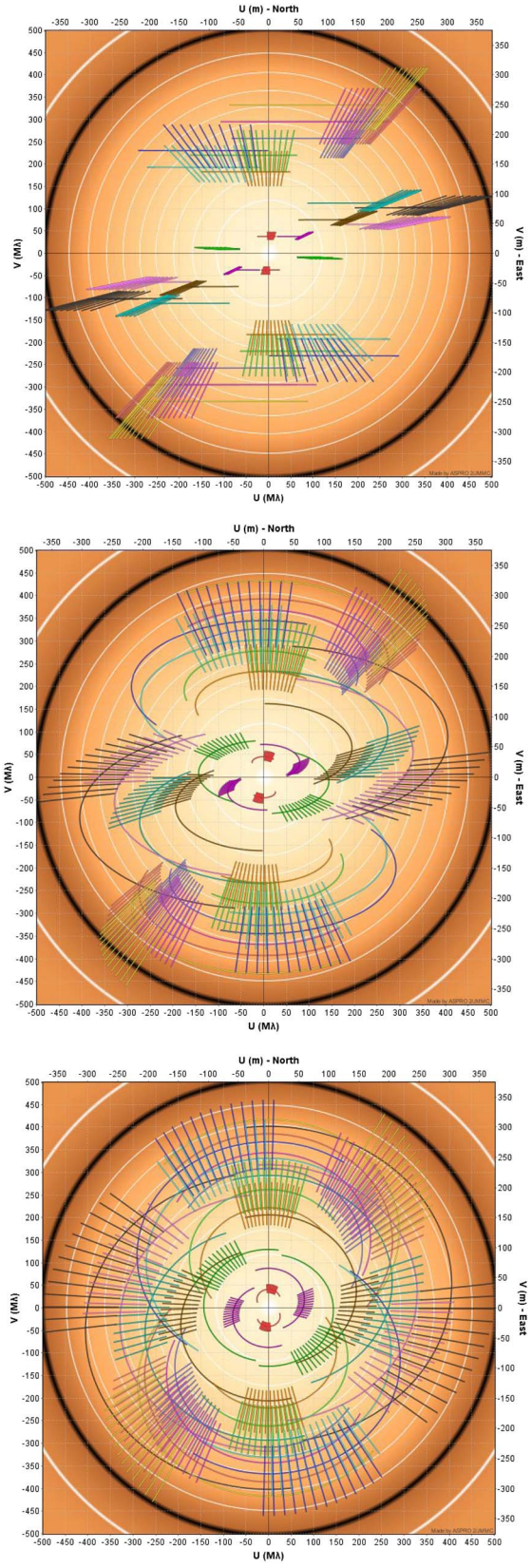

Fig. 4. (U,V) plane coverage for the low-resolution mode of SPICA (50 spectral channels over 300 nm) observing a star with an angular diameter of 0.5 mas and located at three different declinations: 0°, 30°, 60° from top to bottom.

studies (e.g., H α, He, OIII, CaIII lines) at high angular resolution will thus be possible. This mode will be dedicated to spectral imaging of stellar surface and stellar environments. The most critical requirement will be to access reliable measurements of low visibilities and closure phases. In Fig. 5 we present an example of possible spectral imaging reconstruction for the model of ϕ Per [21]. This has been used as model object in the Aspro2 software (available at http://www.jmmc.fr/aspro) configured for a 6T observation with CHARA/SPICA in medium resolution mode. We have considered 32 spectral channels of 0.2 nm around the Hα line, the six telescopes forming 15 baselines for V^2 and 10 triangles for closure phases at seven different times during the night. The image reconstruction has been done with the MIRA software [35]. Pending a more robust performance analysis, a fictive S/N of 10 has been considered on the V^2 measurements for 10 mn of integration. By comparing with Fig. 6 from [21], this figure demonstrates the expected improvement with respect to what has been done with VEGA in 4T mode and with the strong limitations of VEGA in terms of S/N and closure phase determination [21].

In the next subsection, we estimate the performance of SPICA related to the requirements of the science program and the preliminary design that we have presented.

C. Estimation of Performance

As explained in Section 3, today and in the coming years, the only possible solution to reach the angular resolution, the sensitivity and the precision required for our science goals, is to construct a new visible instrument on the CHARA array. The angular resolution has demonstrated the ability to measure angular diameters θ as small as 0.27 mas [30]. Smaller angular diameters give larger squared visibility V^2 with high S/N. The relative precision on the angular diameter $\Delta\theta/\theta$ is classically expressed as

$$\frac{\Delta\theta}{\theta} = \frac{\Delta V}{2J_2(z)}, \tag{1}$$

with ΔV the precision on the visibility measurement, J_2 the Bessel function of order 2, and $z = 15.23B\theta/\lambda$ (B = 300 m is the baseline, $\lambda = 700$ nm the wavelength, and θ the angular diameter expressed in mas). This relation tells us that, for a single measurement, $\Delta\theta/\theta \simeq 10\Delta V$ for $\theta =$ 0.1mas and $\Delta\theta/\theta \simeq 3\Delta V$ for $\theta = 0.2$ mas considering the largest baseline of CHARA. With 6T observations leading to $15V^2$ in one measurement and 50 spectral channels, 750 simultaneous measurements will be collected. So even on a 0.1 mas star a reliable angular diameter could in principle be determined with a relative precision of 1%–2%. It is clear, however, that the measurement of such small angular diameters will not be sensitive to limb darkening and that the absolute calibration will require specific efforts using many (faint) reference stars to reach the required accuracy.

SPICA will benefit from the CHARA AO project that includes an on-telescope full AO system for correcting the atmospheric turbulence and, in the lab, a non-common-path (NCP) error correction with a second deformable mirror. In the CHARA array, each telescope beam encounters over 20 reflections with some of them motorized with continuous motions. Therefore the NCP errors are much greater than on a more

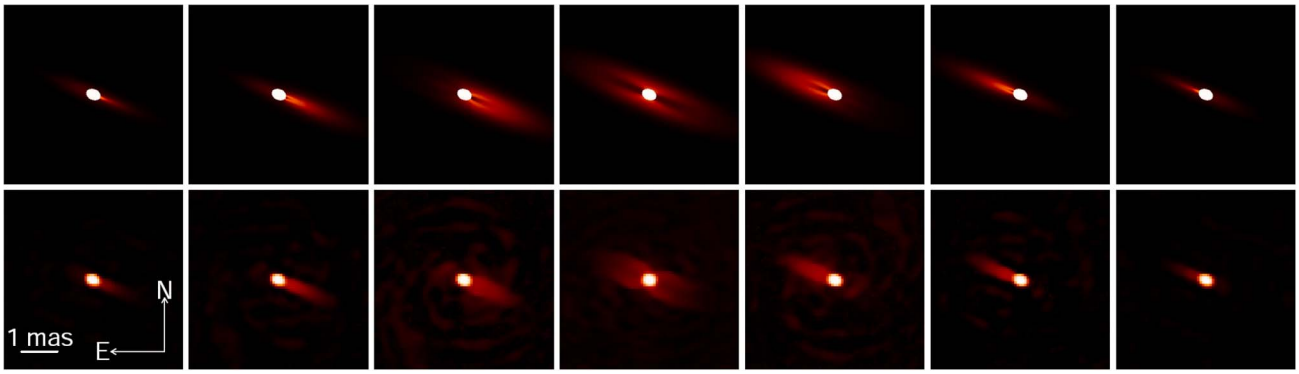

Fig. 5. Input model of a rotating disk in H α for the ϕ Persei star (upper row) and the reconstructed images that SPICA-6T in medium spectral resolution mode could achieve. Each image corresponds to a 0.2 nm spectral band covering from 649 to 663 nm. A S/N of 10 has been considered on the simulated data. These reconstructed images should be compared with the ones produced in [21].

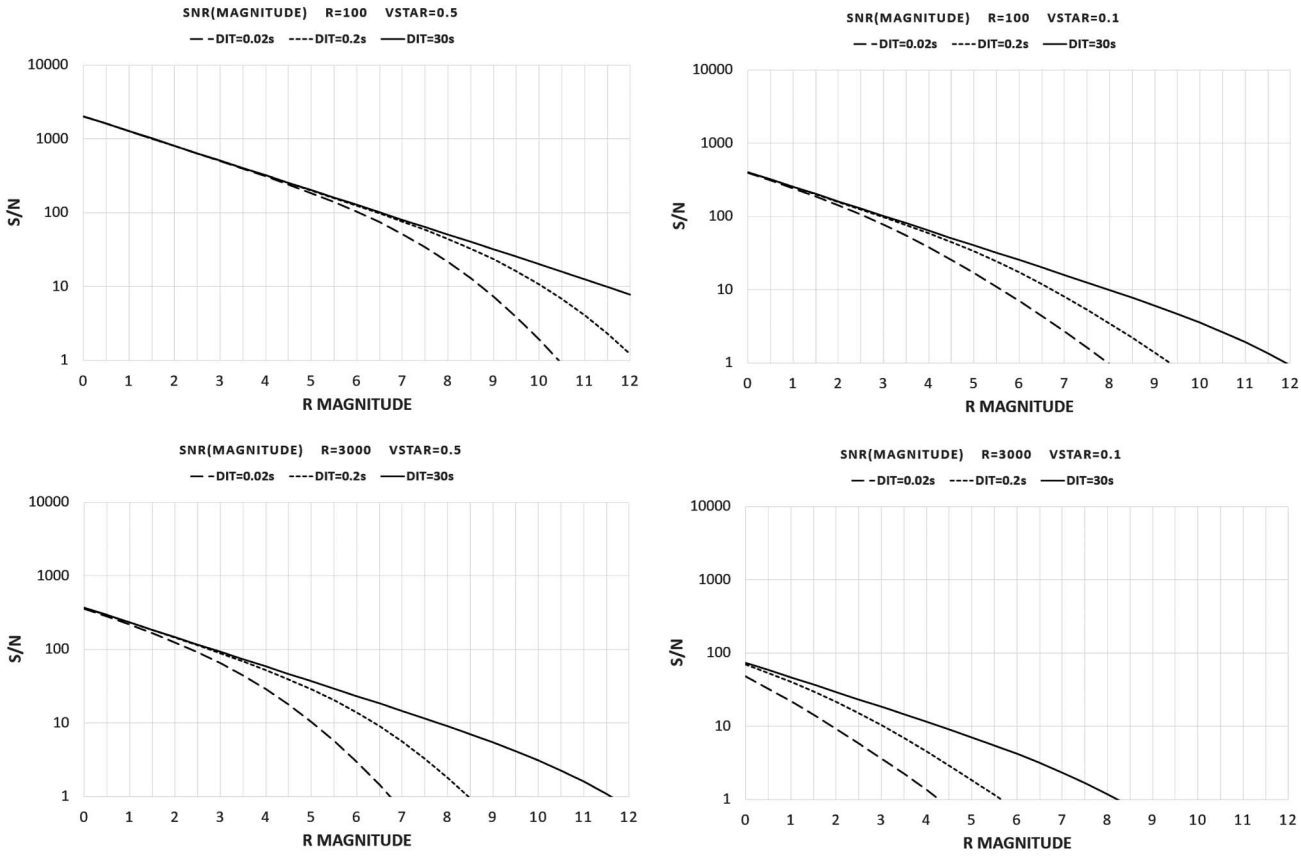

Fig. 6. S/N as a function of magnitude, for three different detector integration time (DIT) of 0.02 ms, 0.2 ms, and 30 s and in four different cases: (top, left) spectral resolution R = 100 and visibility of the star $V_{star} = 0.5$, (top, right) R = 100 and $V_{star} = 0.1$, (bottom, left) R = 3000 and $V_{star} = 0.5$, and (bottom, right) R = 3000 and $V_{star} = 0.1$.

standard AO system on a single telescope. A laser beacon is used to feed the NCP-AO sensors and permit the correction of these slowly changing NCP errors. The NCP-AO system will correct for quasi-static aberrations, track the pupil, correct for lab seeing and tilt, and provide focus and pupil position monitoring for alignment purposes and for correctly feeding the beam combiners.

The CHARA AO systems on the telescopes are designed to reach 83% of Strehl in the H band with median seeing conditions ($r_0 = 12$ cm) [26]. This leads to a 65% coupling efficiency into a single-mode fiber in the H Band. The AO systems will also permit a typical Strehl in the visible of 25%, but it will also provide observing conditions equivalent to current good seeing conditions for 75% of the time. The AO improvement on the flux injection will thus be significant and even more impressive than in the near-IR: from 1% with the tip/tilt only to 25% with the AO.

The precision in the measurement will be given by the principle of spatial filtering, cleaning all the residual modes of the incoming wavefront so that only photometric fluctuations and piston variations are contributing to the noise. (The photometric fluctuations are due to the tip/tilt residual during the injection.) To minimize the measurement noise, an important effort has to be dedicated to the tip/tilt residual at the injection. Photometric channels will be recorded in real time in order to implement full modeling of the interferograms during the data processing. Last but not least, it is clear that the precision will be limited first by photon noise but also by the piston noise. These limitations could be overcome if one has the possibility to increase the exposure time on the detector without blurring the interferometric signal, which means adding a fringe stabilization device. Long exposure time and piston noise are highly related and the solution to reduce these will be to implement a fringe stabilization device. We will see now that reaching a magnitude of 8 in the visible is feasible.

To demonstrate the feasibility of reaching the required precision and sensitivity with the new SPICA instrument, we have used the numerical model of FRIEND [28] to calibrate our S/N estimator on the squared visibility measurements based on an adapted version of the equation provided by Gordon and Buscher [36]:

$$S/N = \frac{\sqrt{N_{SC} * N_f} * \left(\frac{N_{ph} * V_{ins} * V_{star}}{N_{tel}}\right)^2}{\sqrt{\text{PhotonNoise} + \text{ReadNoise} + \text{CoupledTerms}}}, \tag{2}$$

with

$$\text{PhotonNoise} = 2 * (N_{ph} + N_{d+c}) * \left(\frac{N_{ph} * V_{ins} * V_{star}}{N_{tel}}\right)^2 + (N_{ph} + N_{d+c})^2, \tag{3}$$

$$\text{ReadNoise} = N_{pix} * \text{Ron}^2 + (N_{pix} * \text{Ron}^2)^2, \tag{4}$$

$$\text{CoupledTerms} = 2 * N_{pix} * \text{Ron}^2 * \left(\frac{N_{ph} * V_{ins} * V_{star}}{N_{tel}}\right)^2 + 2 * (N_{ph} + N_{d+c}) * N_{pix} * \text{Ron}^2, \tag{5}$$

and where we use the following definitions:

- N_{SC}: the number of spectral channels,
- N_f: the number of frames,
- N_{ph}: the number of photons,
- V_{ins}: the instrumental visibility,
- V_{star}: the target visibility,
- N_{tel}: the number of telescopes,
- N_{d+c}: the number of dark and CIC photons,
- N_{pix}: the number of pixels,
- Ron: the readout noise.

We consider 10 mn of total integration, as this will be considered later to fulfill the science program in a reasonable number of nights. Based on results from FRIEND, we estimate the instrumental visibility V_{ins} to 0.9 and we compute the S/N for a target's visibility V_{star} of 0.5 or 0.1. The calculation is made for a single spectral channel sampled on the detector over 2×300 pixels. We consider the two modes of the instrument with a spectral resolution of 100 and 3000, giving a spectral width of 6 nm and 0.2 nm, respectively, in the considered domain. The characteristics of the noise of the Nüvü512 CCD are considered with a QE of 0.9, a readout noise of 0.1e-, 0.001 CIC events, and 0.0002 dark events per pixel and per frame. To estimate the number of photons we use the calibrated transmission of the CHARA array of 3% in the visible, an instrumental transmission of 0.5, and a 0.7 coefficient corresponding to the 70/30 beam splitter for the photometric channels. The results are presented in Fig. 6.

To estimate the limiting magnitude of the instrument we consider the magnitude giving a S/N of 10 per spectral channel in the various instrumental conditions. As recently demonstrated [28], the optimum detector integration time for the Mount Wilson conditions is 20 ms. The use of the new infrared instruments MIRCx or MYSTIC will permit an efficient group delay tracking in the infrared up to Hmag = 8. Figure 6 demonstrates that in the low resolution mode, dedicated to a program of stellar fundamental parameters, magnitudes of 8.7 ($V = 0.5$) to 5.6 ($V = 0.1$) could be reached for a single spectral channel with a S/N of 10. Considering the simultaneous use of 50 spectral channels covering the 600–900 spectral band and the 15 baselines offered by the six telescopes, this estimation represents a considerable improvement with respect to the VEGA performance ($3V^2$, two or three spectral bands, Rmag 6.5–7). It appears, however, that for measuring low visibilities for well-resolved targets we may be limited. Moreover, it is clear that the performance in medium spectral resolution dedicated to the imaging program is limited and this is particularly true because this imaging program requires reaching low visibilities for dynamical range in the reconstructed images. The only solution we have to push the limiting magnitude is to consider longer exposures to increase the number of photons. To achieve this, we consider two cases where the interferograms are recorded over 200 ms with the assistance of a fringe tracking device and ultimately over 30 s with a fringe tracking system optimized for fast correction and low residual piston noise (around 100 nm rms). With these hypotheses, we can see in Fig. 6 that in the low resolution mode, magnitude 6.7–8 can be reached for $V = 0.1$ and that the imaging program at medium spectral resolution is feasible up to Rmag = 4.3.

These results demonstrate that an instrument such as SPICA could reach its scientific goals for determining precise fundamental stellar parameters and spectral imaging of stellar surfaces and environments. The assistance of a group delay tracking will be guaranteed by the upgraded infrared instruments, so the ultimate performance of SPICA is linked to the development of a fringe tracking device allowing exposures of at least 200 ms in the visible with the goal of reaching long exposures of 30 s. The next section is dedicated to this part of the project.

4. FRINGE TRACKER FOR SPICA

We have demonstrated in the previous section that operating the SPICA instrument with the assistance of a group delay only will limit the performance in magnitude and preclude some of the most important science programs that have been considered.

The main reason resides in the very short exposure time of 20 ms, which is needed to freeze the random motions of the fringe systems due to atmospheric turbulence. Therefore, improving the sensitivity of the instrument through much longer exposure times requires the assistance of a powerful fringe tracker.

During the tests of FRIEND [28], we have shown that an exposure time of 100 ms without any fringe tracker system is possible but at the price of a reduced instrumental visibility degrading the resulting S/N. A first performance improvement is thus to stabilize the fringes over 100–200 ms with an accuracy permitting the preservation of the transfer function, i.e., of the order of 100 nm. Reaching such an accuracy is mainly a question of S/N in the phase calculation of the fringe signal. During the studies for the VLTI second-generation fringe tracker our numerical simulations [37] showed that as long as the photon count is sufficient, reaching this level of accuracy is not an issue. But under a certain threshold of photons per element of measurements (typically 10 photons per sample of the ABCD fringe encoding) the fringe tracking residual starts to increase very rapidly. While sampling the coherence time correctly is important, we also demonstrated that increasing the exposure time of the fringe tracker detector pushes back the magnitude limit under good seeing conditions.

Up to now very few fringe tracking systems have been in operation. The most advanced one is the fringe tracker of the VLTI/Gravity instrument [38]. Expected performance has been studied in detail [39] and actual performance is just being established now during the initial operation of the instrument on the sky. In June 2016, the team announced (ESO Organization Release 1622) their first observation of the S2 star close to Sgr A*, the galactic center, with the use of the star separator and the fringe tracking in operation on the UTs on an off-axis star (GCIRS 16C, Kmag = 9.83). This gives an interesting point of reference to make a reasonable estimation of the possible limiting magnitude of a fringe tracker for the CHARA array. According to the achievements of the GRAVITY instrument, the limiting magnitude of the fringe tracker is defined when one reaches 10 photons per sample of the ABCD fringe encoding, per exposure and per baseline. The main differences to consider are the size of the telescopes (1.8 m for the ATs versus 1 m for CHARA), the number of telescopes (four for the VLTI and six for CHARA), the spectral band for the fringe tracker (K band for Gravity versus H band for CHARA), the difference of transmission (30% for the AT in the K band versus 10% for CHARA in the H band), the difference of coherence time (3 ms for Paranal versus 10 ms for Mount Wilson), and the coupling efficiency (10% for the ATs without AO in the K band versus 65% for the CHARA + AO in H band). For GRAVITY, the requirement on the residual piston is 350 nm but the fringe tracker reaches 100 nm in standard operation (Perrin, private communication). This corresponds to the requirement in the visible and therefore we do not add an additional proportionality factor on the quality of the residual piston. Finally, coupling all these numbers and comparing the expected number of photons per sample permits us to define, as a first approximation based on the GRAVITY experiment, a limiting magnitude of Hmag = 7 for a 6T fringe tracker in the H band on the CHARA array. This estimation is probably optimistic as we neglect in this first approximation the possible decorrelation of the phase in the visible while tracking the phase in the H band. We are planning such phase measurements with FRIEND in the visible together with infrared phase measurements on CHARA to improve this model. Measurements dedicated to the characteristics of the atmospheric turbulence are also foreseen to feed our model of fringe tracking.

5. CONCLUSION

Today, we encounter a very positive situation with the progress made on the FRIEND prototype, the soon-coming AO system on the CHARA telescopes, and the recent successes of the VLTI/GRAVITY instrument. This creates an important opportunity for starting the development of an ambitious instrumental project aiming at producing a six-telescope spectro-interferometer for the CHARA array. This instrument will permit a comprehensive survey of fundamental parameters of stars (radius, effective temperature, mass, and age), from their angular diameters and their limb darkening to detailed surface features. To reach this goal in terms of sensitivity (Rmag $\simeq$ 8), angular resolution (0.1 mas), and precision on the stellar radius ($\Delta R/R \simeq 1\%$), the assistance of a near-infrared fringe tracking device is mandatory. It is important to note that the resolution achievable on the CHARA array at visible wavelengths is 30 times better than ALMA or 10 times better than the E-ELT, and this is mandatory for the SPICA science goals. For a declination larger than −20°, almost 200 stars are within reach of SPICA spectral imaging mode (expected angular diameter between 0.5 and 2 mas, Vmag brighter than 4.5) and for what concerns the angular diameter measurements, almost 10,000 stars enter in the range of SPICA capabilities (expected angular diameter between 0.1 and 3 mas, Vmag brighter than 8). This 10,000-star sample presents the following repartition as a function of the spectral type: O-50, B-1450, A-2340, F-1670, G-1460, K-3090, M-240. The sample includes also 200 stars from the exoplanet encyclopedia catalog (http://exoplanet.eu). The legacy value of this research program will be a reference catalog of modern fundamental parameters of stars with a wide application in general astrophysics, asteroseismology, and exoplanet science.

In the future, a similar instrument should be built for the VLTI. The length of the baselines of the VLTI auxiliary telescopes array is not well adapted for a survey of angular diameters; however, with the advantages of 1 m 80 telescopes and a dense network of interferometric stations, the VLTI equipped with such an instrument could bring a major breakthrough in stellar surface imaging as well as active galactic nuclei studies. These projects will enhance the potential of the current interferometric facilities and will contribute to answering major questions in astrophysics while complementing a large number of "big" space missions. The success of these projects will also depend on the robustness of their operating mode and their capacity of conducting ambitious large programs with a high legacy value.

Funding. Université Côte d'Azur; Centre National de la Recherche Scientifique (CNRS).

Acknowledgment. We wish to warmly thank Guy Perrin for his time in extracting the necessary information to extrapolate the Gravity fringe tracker performance toward a H-band CHARA fringe tracker. This research has made use of the SIMBAD database, operated at CDS, Strasbourg, France, and of the Jean-Marie Mariotti Center Aspro2 service. D. M. warmly thanks the University of Excellence, Université Côte d'Azur, and CNRS/INSU for the funding of this research and especially for offering the possibility of an early purchase of the EMCCD detector.

REFERENCES

1. A. Labeyrie, "Interference fringes obtained on VEGA with two optical telescopes," Astrophys. J. **196**, L71–L75 (1975).
2. M. Shao, M. M. Colavita, B. E. Hines, D. H. Staelin, D. J. Hutter, K. J. Johnston, D. Mozurkewich, R. S. Simon, J. L. Hershey, J. A. Hughes, and G. H. Kaplan, "The Mark III stellar interferometer," Astron. Astrophys. **193**, 357–371 (1988).
3. D. Mourard, I. Tallon-Bosc, F. Rigal, F. Vakili, D. Bonneau, F. Morand, and P. Stee, "Estimation of visibility amplitude by optical long-baseline Michelson interferometry with large apertures," Astron. Astrophys. **288**, 675–682 (1994).
4. J. Davis and W. J. Tango, "The Sydney University 11.4 M prototype stellar interferometer," Proc Astron. Soc. Aust. **6**, 34–38 (1985).
5. J. E. Baldwin, M. G. Beckett, R. C. Boysen, D. Burns, D. F. Buscher, G. C. Cox, C. A. Haniff, C. D. Mackay, N. S. Nightingale, J. Rogers, P. A. G. Scheuer, T. R. Scott, P. G. Tuthill, P. J. Warner, D. M. A. Wilson, and R. W. Wilson, "The first images from an optical aperture synthesis array: mapping of Capella with COAST at two epochs," Astron. Astrophys. **306**, L13–L16 (1996).
6. J. T. Armstrong, D. Mozurkewich, L. J. Rickard, D. J. Hutter, J. A. Benson, P. F. Bowers, N. M. Elias II, C. A. Hummel, K. J. Johnston, D. F. Buscher, J. H. Clark III, L. Ha, L.-C. Ling, N. M. White, and R. S. Simon, "The navy prototype optical interferometer," Astrophys. J. **496**, 550–571 (1998).
7. M. M. Colavita, J. K. Wallace, B. E. Hines, Y. Gursel, F. Malbet, D. L. Palmer, X. P. Pan, M. Shao, J. W. Yu, A. F. Boden, P. J. Dumont, J. Gubler, C. D. Koresko, S. R. Kulkarni, B. F. Lane, D. W. Mobley, and G. T. van Belle, "The Palomar testbed interferometer," Astrophys. J. **510**, 505–521 (1999).
8. A. Glindemann, M. Albertsen, L. Andolfato, G. Avila, P. Ballester, B. Bauvir, F. Delplancke, F. Derie, M. Dimmler, P. Duhoux, E. di Folco, R. Frahm, E. Galliano, B. Gilli, P. N. Giordano, P. B. Gitton, S. Guisard, N. Housen, C. A. Hummel, A. Huxley, R. Karban, P. Kervella, M. Kiekebusch, B. Koehler, S. A. Leveque, T. Licha, A. Longinotti, D. J. McKay, S. Menardi, G. J. Monnet, S. Morel, F. Paresce, I. Percheron, M. Petr-Gotzens, T. Phan Duc, J.-U. Pott, F. Puech, F. T. Rantakyro, A. Richichi, C. Sabet, K. L. Scales, M. Schoeller, N. Schuhler, and M. van den Ancker, M. Vannier, A. Wallander, M. Wittkowski, and R. C. Wilhelm, "VLTI technical advances: present and future," in *Society of Photo-Optical Instrumentation Engineers (SPIE) Conference*, W. A. Traub, ed. (2004), Vol. **5491**, p. 447.
9. M. M. Colavita, G. Serabyn, P. L. Wizinowich, and R. L. Akeson, "Nulling at the Keck interferometer," in *Society of Photo-Optical Instrumentation Engineers (SPIE) Conference Series* (2006), Vol. **6268**.
10. T. A. ten Brummelaar, H. A. McAlister, S. T. Ridgway, W. G. Bagnuolo, Jr., N. H. Turner, L. Sturmann, J. Sturmann, D. H. Berger, C. E. Ogden, R. Cadman, W. I. Hartkopf, C. H. Hopper, and M. A. Shure, "First results from the CHARA array. II. A description of the instrument," Astrophys. J. **628**, 453–465 (2005).
11. J. Armstrong, E. Baines, H. Schmitt, S. Restaino, J. Clark, J. Benson, D. Hutter, R. Zavala, and G. van Belle, "The Navy Precision Optical Interfrometer: an update," in *Society of Photo-Optical Instrumentation Engineers (SPIE) Conference*, Optical and Infrared Interferometry (2016), Vol. **9907**.
12. D. Mourard, J. M. Clausse, A. Marcotto, K. Perraut, I. Tallon-Bosc, P. Bério, A. Blazit, D. Bonneau, S. Bosio, Y. Bresson, O. Chesneau, O. Delaa, F. Hénault, Y. Hughes, S. Lagarde, G. Merlin, A. Roussel, A. Spang, P. Stee, M. Tallon, P. Antonelli, R. Foy, P. Kervella, R. Petrov, E. Thiebaut, F. Vakili, H. McAlister, T. ten Brummelaar, J. Sturmann, L. Sturmann, N. Turner, C. Farrington, and P. J. Goldfinger, "VEGA: visible spEctroGraph and polArimeter for the CHARA array: principle and performance," Astron. Astrophys. **508**, 1073–1083 (2009).
13. D. Mourard, P. Bério, K. Perraut, R. Ligi, A. Blazit, J. M. Clausse, N. Nardetto, A. Spang, I. Tallon-Bosc, D. Bonneau, O. Chesneau, O. Delaa, F. Millour, P. Stee, J. B. Le Bouquin, T. ten Brummelaar, C. Farrington, P. J. Goldfinger, and J. D. Monnier, "Spatio-spectral encoding of fringes in optical long-baseline interferometry. Example of the 3T and 4T recombining mode of VEGA/CHARA," Astron. Astrophys. **531**, A110 (2011).
14. P. Berio, Y. Bresson, J. M. Clausse, D. Mourard, J. Dejonghe, A. Duthu, S. Lagarde, A. Meilland, K. Perraut, I. Tallon-Bosc, N. Nardetto, A. Spang, C. Bailet, A. Marcotto, O. Chesneau, P. Stee, P. Feautrier, P. Balard, and J. L. Gach, "Long baseline interferometry in the visible: the FRIEND project," in *Society of Photo-Optical Instrumentation Engineers (SPIE) Conference*, Optical and Infrared Interferometry IV (2014), Vol. **9146**, p. 914616.
15. M. J. Ireland, A. Mérand, T. A. ten Brummelaar, P. G. Tuthill, G. H. Schaefer, N. H. Turner, J. Sturmann, L. Sturmann, and H. A. McAlister, "Sensitive visible interferometry with PAVO," in *Society of Photo-Optical Instrumentation Engineers (SPIE) Conference Series* (2008), Vol. **7013**.
16. D. Huber, M. J. Ireland, T. R. Bedding, I. M. Brandão, L. Piau, V. Maestro, T. R. White, H. Bruntt, L. Casagrande, J. Molenda-Zakowicz, V. Silva Aguirre, S. G. Sousa, T. Barclay, C. J. Burke, W. J. Chaplin, J. Christensen-Dalsgaard, M. S. Cunha, J. De Ridder, C. D. Farrington, A. Frasca, R. A. García, R. L. Gilliland, P. J. Goldfinger, S. Hekker, S. D. Kawaler, H. Kjeldsen, H. A. McAlister, T. S. Metcalfe, A. Miglio, M. J. P. F. G. Monteiro, M. H. Pinsonneault, G. H. Schaefer, D. Stello, M. C. Stumpe, J. Sturmann, L. Sturmann, T. A. ten Brummelaar, M. J. Thompson, N. Turner, and K. Uytterhoeven, "Fundamental properties of stars using asteroseismology from Kepler and CoRoT and interferometry from the CHARA array," Astrophys. J. **760**, 32 (2012).
17. D. Huber, M. J. Ireland, T. R. Bedding, S. B. Howell, V. Maestro, A. Mérand, P. G. Tuthill, T. R. White, C. D. Farrington, P. J. Goldfinger, H. A. McAlister, G. H. Schaefer, J. Sturmann, L. Sturmann, T. A. ten Brummelaar, and N. H. Turner, "Validation of the exoplanet Kepler-21b using PAVO/CHARA long-baseline interferometry," Mon. Not. R. Astron. Soc. **423**, L16–L20 (2012).
18. T. R. White, D. Huber, V. Maestro, T. R. Bedding, M. J. Ireland, F. Baron, T. S. Boyajian, X. Che, J. D. Monnier, B. J. S. Pope, R. M. Roettenbacher, D. Stello, P. G. Tuthill, C. D. Farrington, P. J. Goldfinger, H. A. McAlister, G. H. Schaefer, J. Sturmann, L. Sturmann, T. A. ten Brummelaar, and N. H. Turner, "Interferometric radii of bright Kepler stars with the CHARA Array: θ Cygni and 16 Cygni A and B," Mon. Not. R. Astron. Soc. **433**, 1262–1270 (2013).
19. J. Sturmann, T. Ten Brummelaar, L. Sturmann, and H. A. McAlister, "Dual three-way infrared beam combiner at the CHARA array," Proc. SPIE **7734**, 77343A (2010).
20. J. D. Monnier, M. Zhao, E. Pedretti, N. Thureau, M. Ireland, P. Muirhead, J.-P. Berger, R. Millan-Gabet, G. Van Belle, T. ten Brummelaar, H. McAlister, S. Ridgway, N. Turner, L. Sturmann, J. Sturmann, D. Berger, A. Tannirkulam, and J. Blum, "Imaging the surface of Altair and a MIRC update," Proc. SPIE **7013**, 701302 (2008).
21. D. Mourard, J. D. Monnier, A. Meilland, D. Gies, F. Millour, M. Benisty, X. Che, E. D. Grundstrom, R. Ligi, G. Schaefer, F. Baron, S. Kraus, M. Zhao, E. Pedretti, P. Berio, J. M. Clausse, N. Nardetto, K. Perraut, A. Spang, P. Stee, I. Tallon-Bosc, H. McAlister, T. ten Brummelaar, S. T. Ridgway, J. Sturmann, L. Sturmann, N. Turner, and C. Farrington, "Spectral and spatial imaging of the Be + sdO binary Φ Persei," Astron. Astrophys. **577**, A51 (2015).
22. D. Mourard, M. Challouf, R. Ligi, P. Bério, J.-M. Clausse, J. Gerakis, L. Bourges, N. Nardetto, K. Perraut, I. Tallon-Bosc, H. McAlister, T. ten Brummelaar, S. Ridgway, J. Sturmann, L. Sturmann, N. Turner, C. Farrington, and P. J. Goldfinger, "Performance, results, and prospects of the visible spectrograph VEGA on CHARA," Proc. SPIE **8445**, 84450K (2012).

23. A. Blazit, X. Rondeau, É. Thiébaut, L. Abe, J.-C. Bernengo, J.-L. Chevassut, J.-M. Clausse, J.-P. Dubois, R. Foy, D. Mourard, F. Patru, A. Spang, I. Tallon-Bosc, M. Tallon, Y. Tourneur, and F. Vakili, "New generation photon-counting cameras: algol and CPNG," Appl. Opt. **47**, 1141–1151 (2008).
24. P. Berio, F. Vakili, D. Mourard, and D. Bonneau, "Removing the photoncentroiding hole in optical stellar interferometry," Astron. Astrophys. **129**, 609–615 (1998).
25. T. ten Brummelaar, X. Che, H. McAlister, M. Ireland, J. Monnier, D. Mourard, S. Ridgway, J. Sturmann, L. Sturmann, N. Turner, and P. Tuthill, "CHARA array adaptive optics II: non-common-path correction and downstream optics," Proc. SPIE **9148**, 91484Q (2014).
26. X. Che, L. Sturmann, J. D. Monnier, T. A. ten Brummelaar, J. Sturmann, S. T. Ridgway, M. J. Ireland, N. H. Turner, and H. A. McAlister, "The CHARA array adaptive optics I: common-path optical and mechanical design, and preliminary on-sky results," Proc. SPIE **9148**, 914830 (2014).
27. J.-L. Gach, P. Balard, E. Stadler, C. Guillaume, and P. Feautrier, "OCAM2: world's fastest and most sensitive camera system for advanced adaptive optics wavefront sensing," in *Second International Conference on Adaptive Optics for Extremely Large Telescopes* (2011), p. 44.
28. M. Martinod, P. Berio, D. Mourard, K. Perraut, A. Meilland, F. Millour, J. M. Clausse, A. Spang, Y. Bresson, J. Dejonghe, C. Bailet, I. Tallon-Bosc, and M. Tallon, "Long baseline interferometry in the visible: first results of the FRIEND project," Proc. SPIE **9907**, 99071H (2016).
29. A. N. Cox, *Allen's Astrophysical Quantities* (Springer, 2000).
30. K. Perraut, S. Borgniet, M. Cunha, L. Bigot, I. Brandão, D. Mourard, N. Nardetto, O. Chesneau, H. McAlister, T. A. ten Brummelaar, J. Sturmann, L. Sturmann, N. Turner, C. Farrington, and P. J. Goldfinger, "The fundamental parameters of the roAp star 10 Aquilae," Astron. Astrophys. **559**, A21 (2013).
31. O. L. Creevey, M. J. P. F. G. Monteiro, T. S. Metcalfe, T. M. Brown, S. J. Jiménez-Reyes, and J. A. Belmonte, "The complementary roles of interferometry and asteroseismology in determining the mass of solar-type stars," Astrophys. J. **659**, 616–625 (2007).
32. M. S. Cunha, C. Aerts, J. Christensen-Dalsgaard, A. Baglin, L. Bigot, T. M. Brown, C. Catala, O. L. Creevey, A. Domiciano de Souza, P. Eggenberger, P. J. V. Garcia, F. Grundahl, P. Kervella, D. W. Kurtz, P. Mathias, A. Miglio, M. J. P. F. G. Monteiro, G. Perrin, F. P. Pijpers, D. Pourbaix, A. Quirrenbach, K. Rousselet-Perraut, T. C. Teixeira, F. Thévenin, and M. J. Thompson, "Asteroseismology and interferometry," Astron. Astrophys. **14**, 217–360 (2007).
33. R. Ligi, D. Mourard, A.-M. Lagrange, K. Perraut, and A. Chiavassa, "Transiting exoplanets and magnetic spots characterized with optical interferometry," Astron. Astrophys. **574**, A69 (2015).
34. B. Lazareff, J.-B. Le Bouquin, and J.-P. Berger, "A novel technique to control differential birefringence in optical interferometers. Demonstration on the PIONIER-VLTI instrument," Astron. Astrophys. **543**, A31 (2012).
35. E. Thiébaut, "MIRA: an effective imaging algorithm for optical interferometry," Proc. SPIE **7013**, 70131I (2008).
36. J. A. Gordon and D. F. Buscher, "Detection noise bias and variance in the power spectrum and bispectrum in optical interferometry," Astron. Astrophys. **541**, A46 (2012).
37. N. Tarmoul, F. Hénault, D. Mourard, J.-B. Le Bouquin, L. Jocou, P. Kern, J.-P. Berger, and O. Absil, "Multi-axial integrated optics solution for POPS, a 2nd-generation VLTI fringe tracker," Proc. SPIE **7734**, 773425 (2010).
38. F. Eisenhauer, G. Perrin, W. Brandner, C. Straubmeier, K. Perraut, A. Amorim, M. Schöller, S. Gillessen, P. Kervella, M. Benisty, C. Araujo-Hauck, L. Jocou, J. Lima, G. Jakob, M. Haug, Y. Clénet, T. Henning, A. Eckart, J.-P. Berger, P. Garcia, R. Abuter, S. Kellner, T. Paumard, S. Hippler, S. Fischer, T. Moulin, J. Villate, G. Avila, A. Gräter, S. Lacour, A. Huber, M. Wiest, A. Nolot, P. Carvas, R. Dorn, O. Pfuhl, E. Gendron, S. Kendrew, S. Yazici, S. Anton, Y. Jung, M. Thiel, É. Choquet, R. Klein, P. Teixeira, P. Gitton, D. Moch, F. Vincent, N. Kudryavtseva, S. Ströbele, S. Sturm, P. Fedou, R. Lenzen, P. Jolley, C. Kister, V. Lapeyrére, V. Naranjo, C. Lucuix, R. Hofmann, F. Chapron, U. Neumann, L. Mehrgan, O. Hans, G. Rousset, J. Ramos, M. Suarez, R. Lederer, J.-M. Reess, R.-R. Rohloff, P. Haguenauer, H. Bartko, A. Sevin, K. Wagner, J.-L. Lizon, S. Rabien, C. Collin, G. Finger, R. Davies, D. Rouan, M. Wittkowski, K. Dodds-Eden, D. Ziegler, F. Cassaing, H. Bonnet, M. Casali, R. Genzel, and P. Lena, "GRAVITY: observing the universe in motion," Messenger **143**, 16–24 (2011).
39. E. Choquet, J. Menu, G. Perrin, F. Cassaing, S. Lacour, and F. Eisenhauer, "Comparison of fringe-tracking algorithms for single-mode nearinfrared long-baseline interferometers," Astron. Astrophys. **569**, A2 (2014).